arXiv:hep-ph/0410106v2 10 Nov 2004

Proceedings of the DIS'2004, Štrbské Pleso, Slovakia

SUMMARY OF WORKING GROUP B: DIFFRACTION AND VECTOR MESONS

ALESSIA BRUNI[1], MARKUS DIEHL[2], FRANK-PETER SCHILLING[2]

1. INFN Bologna, I-40156 Bologna, Italy
2. Deutsches Elektronen-Synchroton DESY, D-22603 Hamburg, Germany
E-mails: alessia@mail.desy.de, mdiehl@mail.desy.de, fpschill@mail.desy.de

We summarise the contributions presented in working group B: "Diffraction and Vector Mesons".

1 Introduction

The understanding of diffractive lepton-hadron or hadron-hadron interactions at high energies, where at least one of the beam hadrons stays intact and loses only a small fraction of its incident momentum, still represents one of the main challenges in Quantum Chromodynamics. Diffraction is being extensively studied both at HERA and the TEVATRON, and there is a growing community planning to continue this research at the LHC.

The current experimental data as well as future plans have been reviewed during the sessions in Working Group B, where in total 21 experimental talks were presented. There were 19 theoretical talks, 11 of which dealt with the topic of saturation. In the following, contributions will be summarised which cover diffraction at HERA (section 2) and the TEVATRON (section 3), vector meson production and DVCS (section 4), the phenomenology of saturation (section 5), and future experimental opportunities (section 6).

2 Diffraction at HERA

2.1 Inclusive Diffraction

In diffractive deep-inelastic scattering at HERA (Figure 1) the virtual photon γ^* emitted from the beam electron provides a point-like probe to study the structure of the diffractive exchange, similarly to ordinary DIS probing proton structure. Experimentally, diffractive events are identified either by tagging the elastically scattered proton in *Roman pot* spectrometers $60 - 100$ m downstream from the interaction point or by properties of the hadronic final state, for example by a large rapidity gap without particle production between a central hadronic system and the proton beam direction. The diffractive *reduced cross section* $\sigma_r^{D(4)}$ is defined as

$$\frac{d^4\sigma^{ep\to eXp}}{dx_{I\!P}\; dt\; d\beta\; dQ^2} = \frac{2\pi\alpha^2 Y_+}{\beta Q^4}\sigma_r^{D(4)}(x_{I\!P}, t, \beta, Q^2)\ . \tag{1}$$

Here $x_{I\!P}$ is the longitudinal momentum loss of the incident proton, t is the squared four-momentum transfer at the proton vertex, β is the momentum fraction of the

© Institute of Experimental Physics SAS, Košice, Slovakia

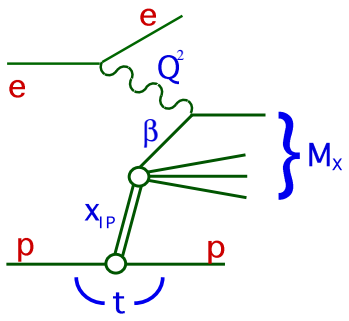

Figure 1. Illustration of a diffractive DIS event.

quark struck by the photon with respect to the diffractive exchange (i.e. the equivalent of x in ordinary DIS), and Q^2 is the photon virtuality. One further has $Y_+ = 1 + (1-y)^2$ in terms of the usual inelasticity variable y. The reduced cross section $\sigma_r^{D(4)}$ is related to the diffractive structure functions F_2^D and F_L^D by $\sigma_r^D = F_2^D - (y^2/Y_+)F_L^D$. Except at the highest values of y, one has $\sigma_r^D = F_2^D$ to a very good approximation. If the outgoing proton is not detected, the measurements are integrated over t, i.e. $\sigma_r^{D(3)}(x_{I\!P}, \beta, Q^2) = \int \mathrm{d}t\ \sigma_r^{D(4)}(x_{I\!P}, t, \beta, Q^2)$.

Both H1 and ZEUS [1,2] have presented recent precise measurements of $\sigma_r^{D(3)}$. The H1 measurement selects diffractive events by requiring a large rapidity gap and covers low, medium and high Q^2, with $1.5 < Q^2 < 1600$ GeV^2 and $x_{I\!P} < 0.05$ [3]. The data are consistent with measurements using the H1 Forward Proton Spectrometer FPS to tag the diffractively scattered proton directly [4]. ZEUS selected diffractive events by using both the so-called "M_X method" ($2.2 < Q^2 < 80$ GeV^2) and the Leading Proton Spectrometer LPS ($0.03 < Q^2 < 100$ GeV^2) [5]. The ZEUS LPS data cover a large range in $x_{I\!P}$ up to 0.1, a region relevant for the comparison with the Tevatron data (see section 3).

The H1 and ZEUS data exhibit clear positive Q^2 scaling violations indicative of a large gluonic contribution to the exchange (see Figures 2 and 3). The ratio of the diffractive to the inclusive DIS cross section is observed to be flat except at the highest β. For $Q^2 \gtrsim 10$ GeV^2, the $x_{I\!P}$ dependence of the cross section can be parameterized in terms of an effective Pomeron intercept $\alpha_{I\!P}(0) \sim 1.2$, which is significantly larger than the soft Pomeron value of 1.08. Resolving the issue of a possible variation of $\alpha_{I\!P}(0)$ with Q^2 in inclusive diffractive DIS needs further experimental input.

Applying the QCD factorization theorem for diffractive DIS [6]:

$$\frac{\mathrm{d}^2\sigma(x, Q^2, x_{I\!P}, t)^{\gamma^* p \to pX}}{\mathrm{d}x_{I\!P}\ \mathrm{d}t} = \sum_i \int_x^{x_{I\!P}} \mathrm{d}z\ \hat{\sigma}^{\gamma^* i}(x, Q^2, z)\ p_i^D(z, Q^2, x_{I\!P}, t)\ , \qquad (2)$$

both collaborations have performed next-to-leading order (NLO) QCD fits to their diffractive DIS data [1,2]. The NLO diffractive parton distributions p_i^D extracted from the H1 data are shown in Figure 4 (they will be referred to as H1 2002 fit in the following). The shape of the diffractive PDFs extracted by ZEUS is less well

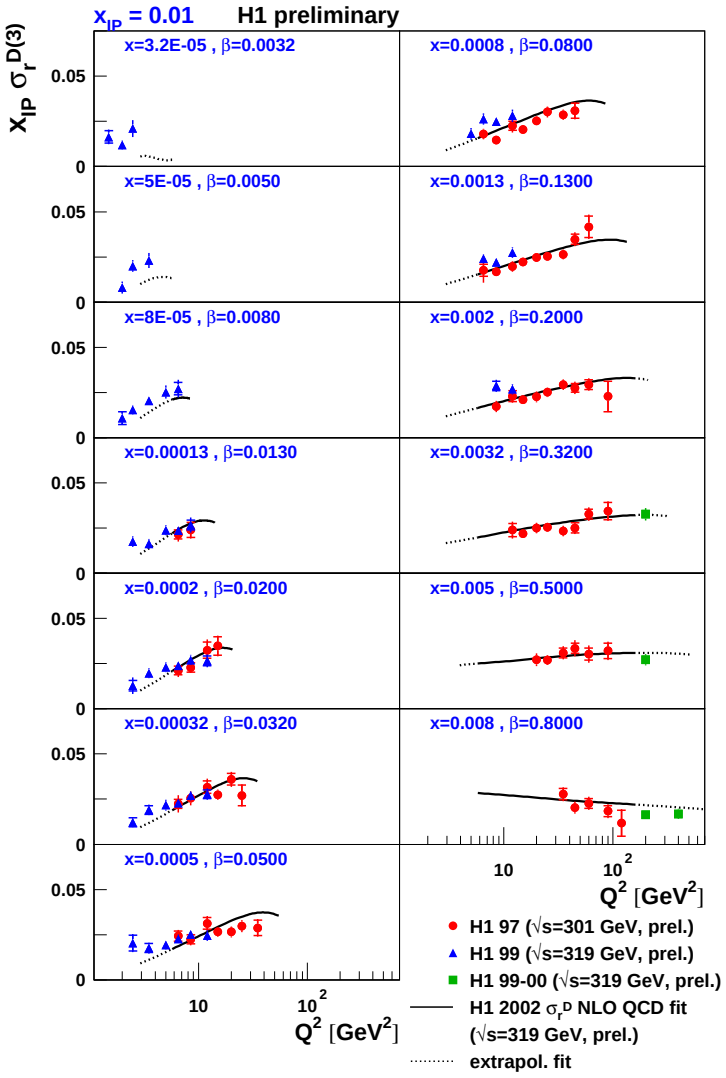

Figure 2. H1 measurements of the Q^2 dependence of $x_{I\!P}\,\sigma_r^{D(3)}$.

constrained (only the statistically limited LPS data with $x_{I\!P} < 0.01$ were used), but using in addition diffractive charm data [7] further constrains the diffractive gluon distribution. In the fits of both H1 and ZEUS, the momentum fraction of the diffractive exchange carried by gluons is determined to be about 80% to 85%. The diffractive PDFs can be used to test QCD factorization in diffraction by predicting jet and charm cross sections (sections 2.2 and 3).

At the workshop, ZEUS has reported the observation of events with a large rapidity gap in charged current interactions at high Q^2 [8]. In 61 pb^{-1} of data, 9

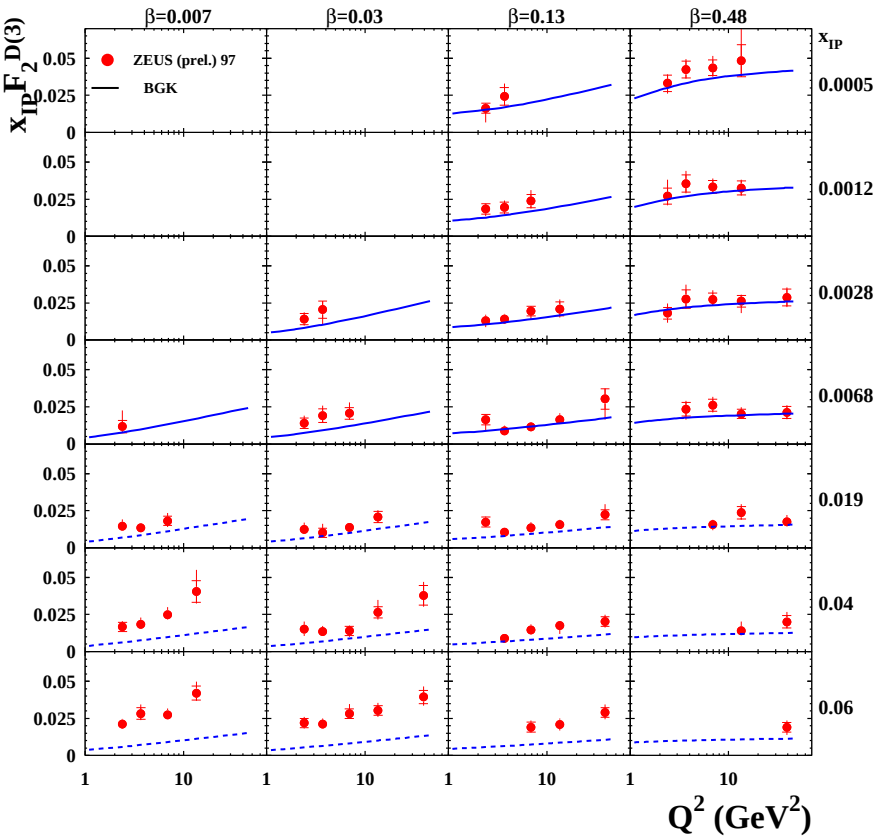

Figure 3. ZEUS measurements of the Q^2 dependence of $x_{I\!P}\, F_2^{D(3)}$.

events are observed for $Q^2 > 200$ GeV^2 and $x_{I\!P} < 0.05$, corresponding to a cross section of $\sigma^{\mathrm{cc-D}} = 0.49 \pm 0.20(\mathrm{stat.}) \pm 0.13(\mathrm{syst.})$ pb, see Figure 5. With the Monte Carlo RAPGAP and the H1 2002 diffractive PDFs, one expects 5.6 events over a background of 2.1 events.

ZEUS has also presented [9] a measurement of leading neutron production for $Q^2 \sim 0$ in the kinematic range $0.05 < |t| < 0.425$ GeV^2 and $0.6 < x_L < 0.925$, where $x_L = E_n/E_p$ [10]. Within the reggeised one-pion exchange model, the data have been used to extract the slope of the pion trajectory as $\alpha'_\pi = 1.39 \pm 0.16 \pm 0.26$ GeV^{-2}, supporting the applicability of this model in the reaction $\gamma p \to nX$. Results were also presented [9] on measurements of DIS with a leading proton [11].

2.2 Diffractive Final States

Since QCD hard scattering factorization holds for diffractive DIS, calculations based on diffractive PDFs extracted from inclusive measurements of $\sigma_r^{D(3)}$ can predict cross sections for diffractive final states such as dijets or charm production. How-

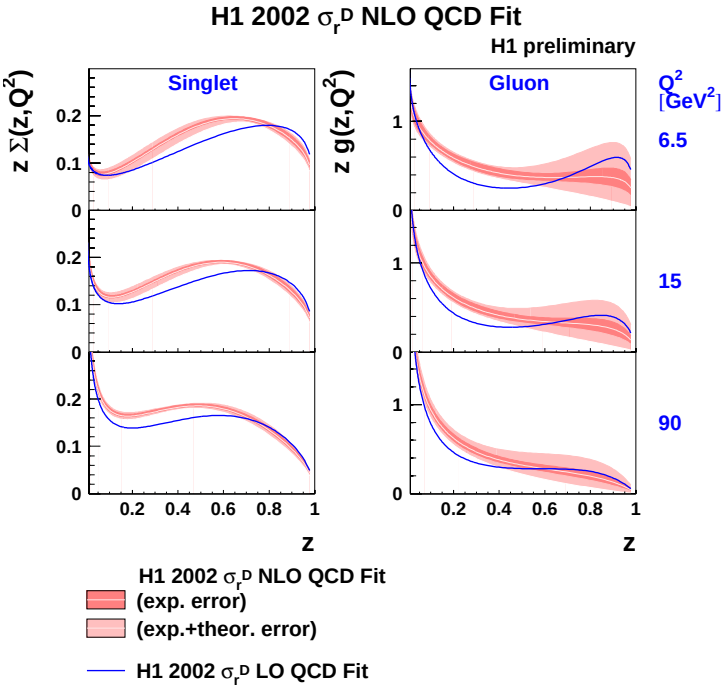

Figure 4. Diffractive parton distributions obtained from the H1 NLO QCD fit.

ever, the factorization proof of Collins [6] does not hold in the case of photoproduction, where the photon is quasi-real ($Q^2 \sim 0$) or in the case of diffractive hadron-hadron scattering.

In fact, it has been known for a few years that diffractive PDFs extracted from HERA data overestimate the rate of diffractive dijet events at the TEVATRON by one order of magnitude [12]. This breakdown of factorization can be attributed to additional soft interactions between the beam hadrons and their fragments. Such interactions explicitly appear in the analysis of the factorization theorems: they cancel out in $\gamma^* p$ processes but not in hadron-hadron collisions [6]. They are expected to reduce the rate of observed diffractive events (*rapidity gap survival probability*) and have been modeled in soft physics approaches. It is thus interesting to study at HERA the rate of diffractive dijet photoproduction events, since the real photon can act similarly to the second hadron in $p\bar{p}$ collisions.

At the workshop, H1 has presented [13] new results on comparisons between dijet and charm production in diffractive DIS with predictions based on the H1 2002 diffractive PDFs (Figure 4). An important development is that these comparisons are now done by calculating the hard cross sections to NLO accuracy, i.e. to the same precision as in standard DIS. The diffractive dijet cross section for $4 < Q^2 < 80$ GeV^2, $x_{I\!P} < 0.05$ and $p_{T,jet}^{1(2)} > 5(4)$ GeV is shown in Figure 6(a), compared with NLO calculations based on the H1 NLO diffractive PDFs. Good agreement is observed, in support of QCD factorization. Similar conclusions can be drawn from

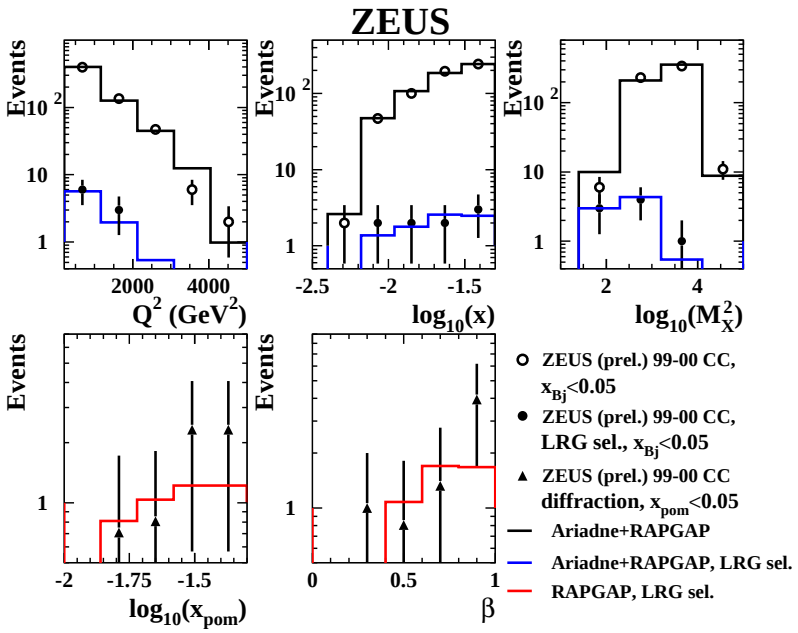

Figure 5. Distributions for charged current events with and without a large rapidity gap as observed by ZEUS.

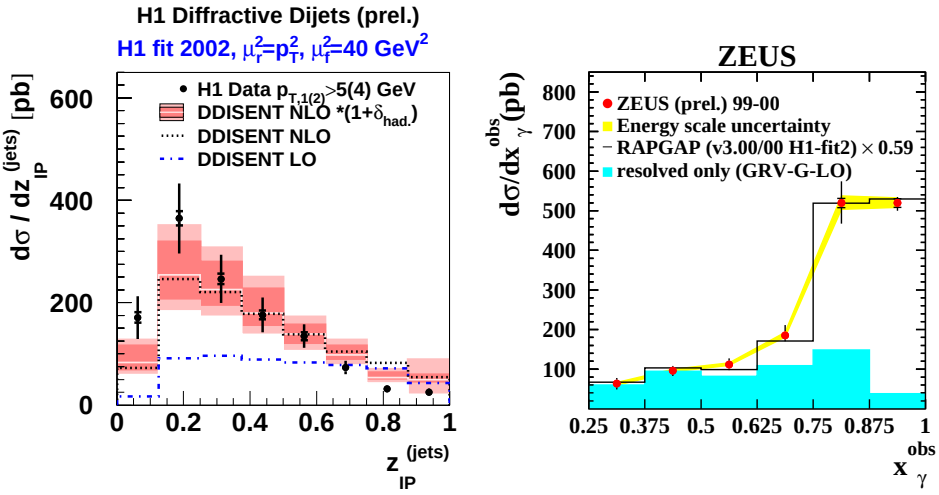

(a) (b)

Figure 6. (a) H1 diffractive DIS dijet cross section, compared with NLO calculations. (b) ZEUS diffractive dijet cross section in photoproduction, compared with LO calculations.

the study of diffractive charm production in DIS, presented by both H1 [13,14] and ZEUS [15,16] .

In the case of diffractive dijet photoproduction, both HERA collaborations have presented very interesting results: ZEUS has shown [17] new cross section measurements in the kinematic range $Q^2 < 1$ GeV^2, $x_{I\!P} < 0.035$ and $p_{T,jet}^{1(2)} > 7.5(6.5)$ GeV (Figure 6(b)). The measurements are compared with the leading order (LO) Monte Carlo program RAPGAP using the previous H1 fits 2 and 3 of diffractive PDFs [18]. Good agreement in both shape and normalization is achieved if the prediction is scaled by a factor 0.6. In contrast, H1 [13,19] finds good agreement at LO without having to rescale the prediction when the more recent H1 2002 diffractive PDFs [3] are used. The two results are not contradicting each other, given that the diffractive gluon distribution in the H1 2002 fit is smaller than in the previous H1 fits 2 or 3 by a factor similar to the rescaling factor 0.6 needed in the ZEUS analysis. When comparing photoproduction dijet data with LO calculations using the 2002 diffractive PDFs from H1, both the ZEUS and H1 results are thus consistent with a rapidity gap survival probability close to 1, in contrast to the findings at the TEVATRON.

Kramer [20] has presented an analysis of diffractive dijet photoproduction at NLO, using the diffractive PDFs from the new H1 NLO analysis as an input. Compared with the H1 data, the calculation is found to give too large a cross section. Agreement with the data is found when introducing a suppression factor of 0.34 for the *resolved* photon part in the calculation (whose value was taken from a model evaluation of the gap survival probability for this process in [21]). After this conference, both H1 and ZEUS have presented comparisons of their measurements with NLO calculations and found that a *global* suppression factor is required to describe the data, i.e. a suppression of both the resolved and the direct photon part [22,23]. The origin of the discrepancy between these different studies remains to be clarified, as well as their relation with the comparisons at LO.

In a further contribution to the workshop, results from ZEUS [24] on the process $\gamma\gamma \to \mu\mu$ were presented [25], which are sensitive to the electromagnetic light-cone wave function of the photon.

3 Diffraction at the TEVATRON

Results on diffraction at the TEVATRON were presented at the workshop in two contributions by the CDF [26] and D0 [28] collaborations.

CDF [26] has determined the ratio of single-diffractive to non-diffractive dijet events [12] for $p_{T,jet} > 7$ GeV and $0.035 < x_{I\!P} < 0.095$, which is found to be one order of magnitude smaller than what is expected using the diffractive PDFs from HERA. These results are consistent with CDF studies of diffractive J/Ψ production. However, the ratio of double- to single-diffractive dijets is found to be about a factor 5 larger than the ratio of single- to non-diffractive dijets, suggesting that there is at most a small extra suppression when going from one to two rapidity gaps in the event.

Within the approach of Good and Walker to diffraction, Bialas [27] has shown that in fact there is no suppression when going from one to two gaps in models

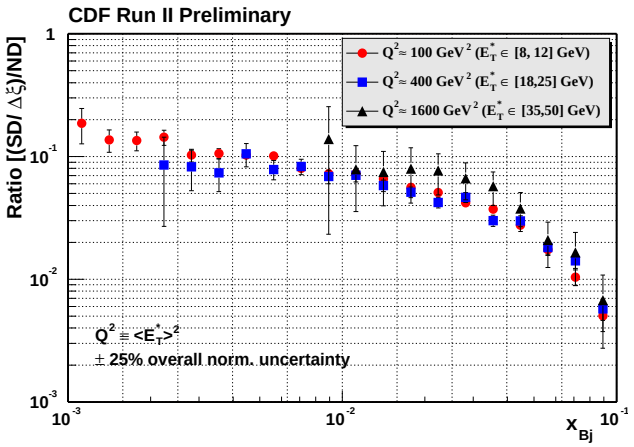

Figure 7. Ratio of single- to non-diffractive dijet production from CDF.

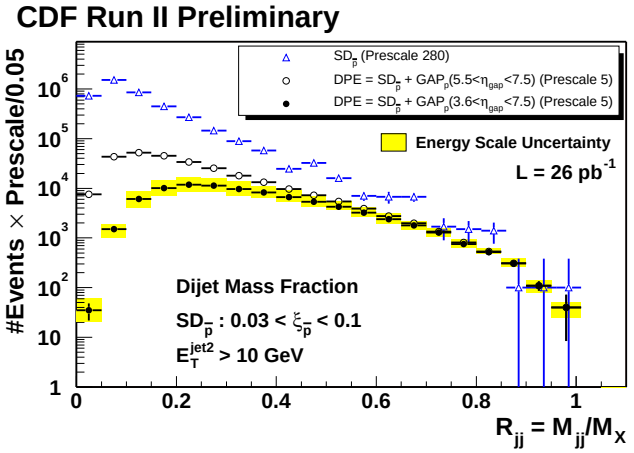

Figure 8. Fractional invariant mass contained in the dijet system for single- and double-diffractive events from CDF.

where the interactions responsible for factorisation breaking are restricted to purely elastic scattering (neglecting e.g. interactions involving proton dissociation, which are included in more refined approaches).

With new detectors ("MiniPlug Calorimeter") added to the existing Roman Pot devices, CDF has now improved capabilities for detecting diffractive events in Run II. Using the new Run II data, CDF could reproduce the results obtained in Run I. In addition, the jet measurement is now performed in several $p_{T,jet}$ intervals (Figure 7). The ratio of single- to non-diffractive dijets shows no significant p_T^2

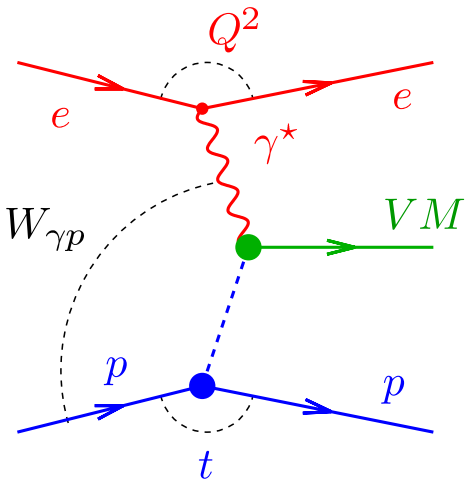

Figure 9. Diagram of elastic vector meson production at HERA.

dependence in the range $100 < p_T^2 < 1600$ GeV^2.

Run II data are also being used by CDF to search for exclusive dijet (Figure 8) and χ_c production in double diffractive events, with first results presented at this workshop. The measurement of the cross sections of these processes is considered to provide important calibration points necessary to normalize model predictions for diffractive Higgs production at the LHC (see section 6).

In contrast to Run I, the D0 detector includes Roman Pot spectrometers in Run II [28]. The outgoing beam pipes for both p and $\bar{p}$ are equipped with in total 9 spectrometers composed of 18 Roman Pots. The new detectors have been used for an initial measurement of the elastic t slope and are expected to provide a wealth of diffractive data.

4 Vector Meson Production and DVCS

In a joint session of the diffractive and the spin working group, vector meson production and deeply virtual Compton scattering (DVCS) were discussed. Contributions from HERMES to this session [29,30] are summarised in [31].

Diffractive vector meson production at HERA, $e + p \to e + V + Y$, where V is the vector meson and Y is either a proton ("elastic") or a low-mass proton dissociation system, provides a clean laboratory to study the dynamics of diffraction, in particular the transition from soft to hard QCD. Several different scales are present in this process, such as the γp centre-of-mass energy W, the photon virtuality Q^2, the squared four-momentum transfer t at the proton vertex, and the mass m_V of the vector meson, which can all be tuned in the measurement (Figure 9). In a non-perturbative description, the photon fluctuates into a vector meson that scatters on the proton via soft Pomeron exchange, which predicts the energy dependence of the γp cross section to be $W^{4(\alpha_{I\!P}(t)-1)} \sim W^{0.22}$. This approach is able to describe

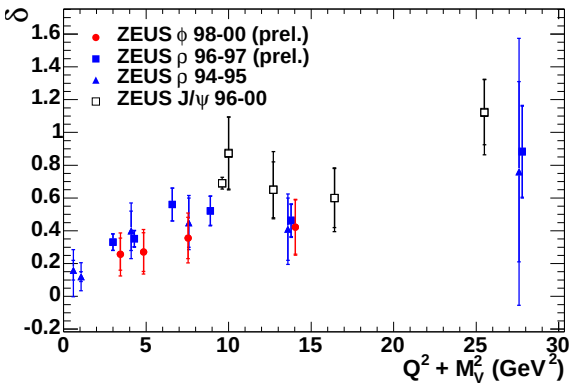

Figure 10. W^δ dependence vs. $Q^2 + m_V^2$ for elastic vector meson production from ZEUS.

the data for light vector mesons if both Q^2 and t are small. In the presence of a hard scale Q^2 or m_V, perturbative QCD approaches based on two-gluon exchange predict a stronger rise of the cross section with energy $W^2 \sim 1/x$, corresponding to the small-x rise of the gluon density in the proton.

ZEUS has presented [32] new high statistics results on exclusive ϕ production in DIS in the kinematic range $2 < Q^2 < 70$ GeV^2, $35 < W < 145$ GeV and $|t| < 0.6$ GeV^2. The energy dependence W^δ is observed to become steeper with Q^2: δ increases from 0.26 ± 0.10 at $Q^2 = 2.4$ GeV^2 to 0.42 ± 0.16 at $Q^2 = 13$ GeV^2. Thus, a picture emerges that at around $Q^2 \sim m_{J/\Psi}^2 \sim 10$ GeV^2 the energy dependence of the light vector mesons ρ and ϕ becomes similar to the one of the J/Ψ at $Q^2 \sim 0$ (Figure 10), suggesting that $\mu^2 \sim Q^2 + m_V^2$ could play the role of a universal scale in this process. Furthermore, from the W dependence measured in different t intervals, the slope parameter of the Pomeron trajectory $\alpha'_{I\!P}$ was extracted and found to be consistent with zero, in contrast with the soft Pomeron model. ZEUS has also measured the Q^2 dependence of the exponential t slope parameter b, where some indication for a decrease with Q^2 is observed.

Diffractive J/Ψ production involves the charm quark mass as a hard scale. This allows for a description in terms of hard-scattering factorization and makes the process sensitive to the generalized gluon distribution. ZEUS [33] has presented comprehensive results on J/Ψ production [34] for $0 < Q^2 < 100$ GeV^2 and $30 < W < 220$ GeV. In particular, cross sections as a function of W and Q^2 have been measured and compared with calculations based on two-gluon exchange. The results exhibit a strong sensitivity to the choice of gluon distribution in the calculation (Figure 11). The Pomeron trajectory at $Q^2 = 7$ GeV^2 was extracted as $\alpha_{I\!P}(t) = (1.20 \pm 0.03) + (0.07 \pm 0.05)t$, which is substantially different from the soft Pomeron for both intercept and slope.

Szymanowski [35] has a presented the first NLO calculation for exclusive J/Ψ photoproduction [36] and for electroproduction of light vector mesons in the framework of leading-twist collinear factorization. The dependence of the NLO result on the factorization and renormalization scales is smaller than at LO, as is generally

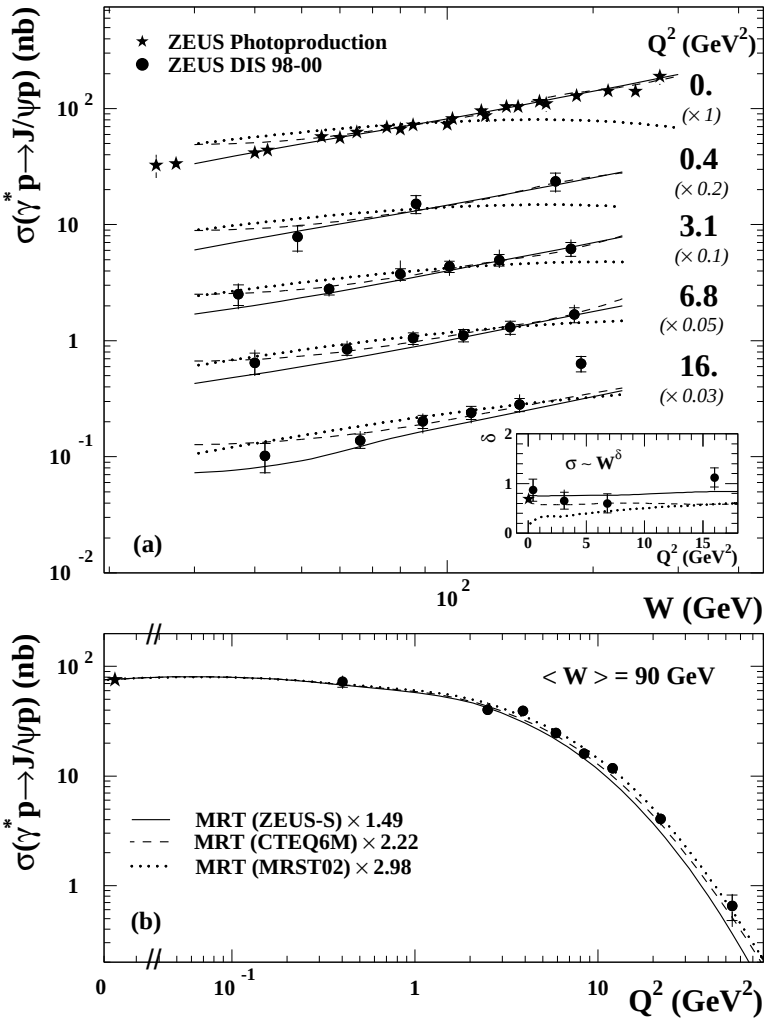

Figure 11. J/Ψ cross section dependence on W and Q^2 from ZEUS. The different curves correspond to different gluon densities (see key in lower panel) used to model the generalized gluon distribution.

expected. The size of the NLO corrections in J/Ψ production is found to be substantial over a large kinematic range. The origin of this is currently not understood and further study is needed. One may speculate that the situation is better for J/Ψ electroproduction at sufficiently large Q^2, but an NLO calculation of this process is presently not available.

J/Ψ photoproduction with proton dissociation at high $|t|$ receives particular interest, because it offers a test of BFKL dynamics in the exchanged gluon ladder. Both H1 and ZEUS have presented [37] results on J/Ψ production going up to large values of $|t|$ [38,39]. H1 has measured the cross section for $\gamma p \to J/\Psi\, Y$

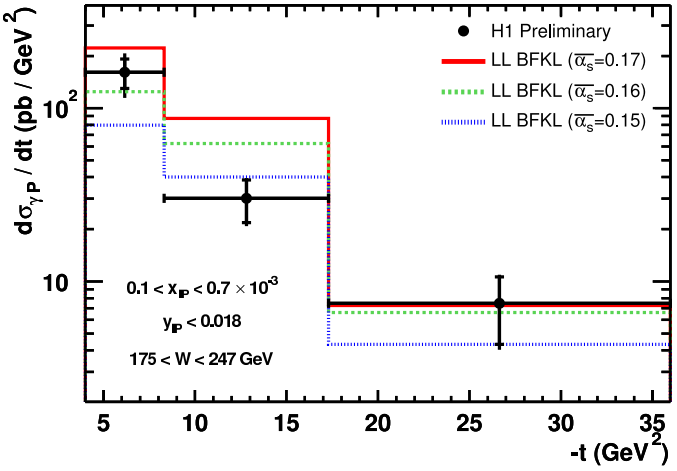

Figure 12. Diffractive high-$|t|$ photon production cross section from H1.

up to $|t| = 25$ GeV^2 and found a power law behaviour in t of $d\sigma/dt \sim |t|^{-3.0\pm0.1}$. A BFKL calculation including an estimate of next-to-leading corrections is in reasonable agreement with the H1 and ZEUS data. However, the agreement becomes worse if effects of the running of α_s are included. Motyka [40] has presented a detailed theoretical study of vector meson photoproduction at large t in the BFKL framework, including the meson polarization [41].

An even simpler process to look for effects of BFKL evolution is high-$|t|$ photon production $\gamma p \to \gamma Y$, which does not involve a vector meson wave function. H1 has presented [37] the first cross section measurement of this process in photoproduction [42], reaching $|t| < 35$ GeV^2 (Figure 12). The data are qualitatively described by a leading-log BFKL calculation.

Deeply virtual Compton scattering (DVCS), i.e. exclusive photon production $\gamma^* p \to \gamma p$ at small $|t|$ but large Q^2, provides an opportunity to obtain information about generalized parton distributions (GPDs). Since the DVCS final state is indistinguishable from the final state of the Bethe-Heitler process, where the photon is radiated from the lepton, the amplitudes of the two processes add coherently. The resulting interference term is estimated to be negligible in the kinematics of H1 and ZEUS, as long as the measurement integrates over the azimuthal angle between the lepton and the hadron plane [43]. H1 and ZEUS have extracted DVCS cross sections by subtracting the calculated Bethe-Heitler cross section from the measured data [44,45].

H1 has presented [46] new results on the DVCS [47] cross section for $4 < Q^2 < 80$ GeV^2, $30 < W < 140$ GeV and $|t| < 1.0$ GeV^2 (Figure 13). The measured cross sections as functions of Q^2 or W are in reasonable agreement with previous results from H1 and ZEUS. They are compared with NLO QCD calculations using GPD parameterizations based on the CTEQ6 and MRST2001 PDFs, as well as with colour dipole models. All models describe the data within the uncertainties

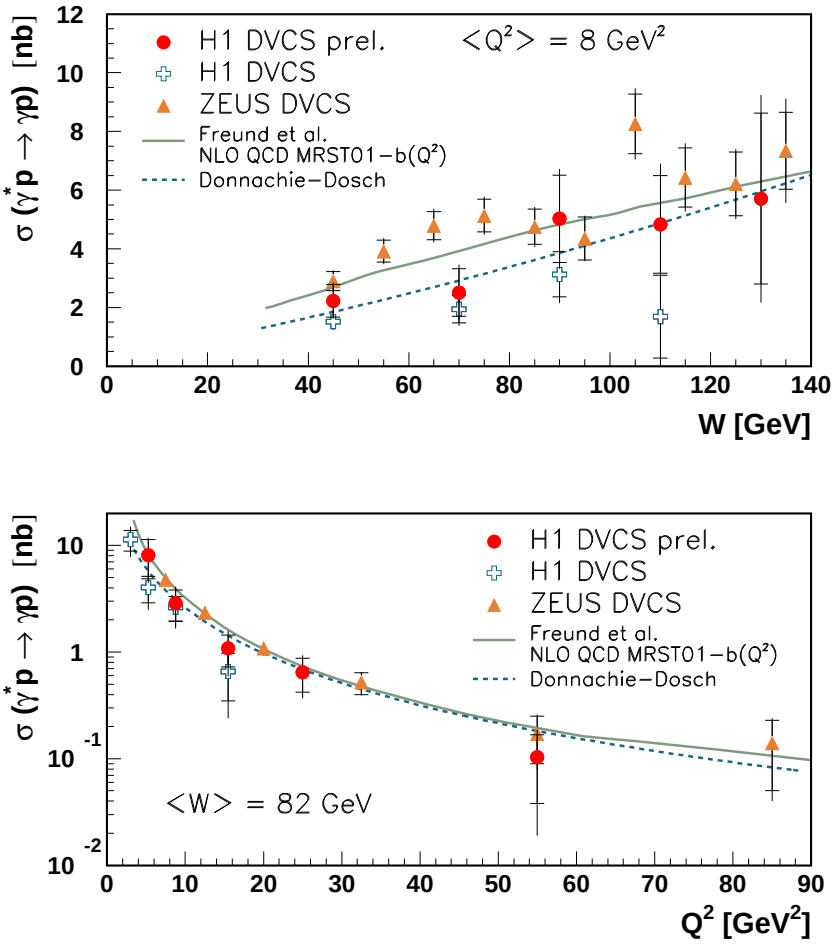

Figure 13. DVCS cross section data compared with calculations in the framework of generalized parton distributions (Freund et al.) or of the dipole formulation (Donnachie and Dosch).

if the t slope parameter is taken to be $b = 7$ GeV^{-2}. To constrain the models further, it is necessary to measure the t-dependence of the DVCS cross section. This became also manifest in the presentation by Favart [48], who compared the results of several saturation models for DVCS: the present uncertainty in the cross section due to the unknown t dependence is in fact of similar size as the variation of different models for saturation effects.

The t dependence of DVCS and of exclusive vector meson production has been a recurring theme at the workshop, with a dedicated presentation by Weiss [49]. By a Fourier transform it can be translated into information in the impact parameter plane. In the leading-twist formalism, the Fourier transform of generalized parton

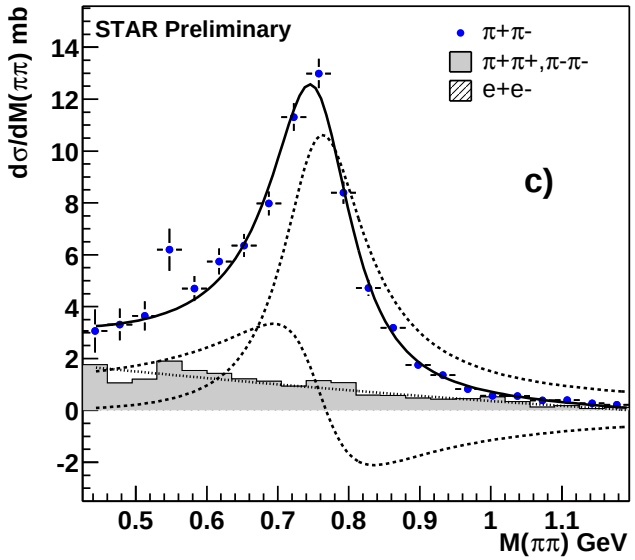

Figure 14. ρ^0 peak in the $\pi\pi$ invariant mass spectrum from Au+Au collisions at STAR.

distributions gives the transverse distance of the struck parton from the proton center. In the dipole formulation of the leading order BFKL formalism, the Fourier transform of the scattering amplitude with respect to t gives the distance from the proton center where the dipole scatters off gluons in the target. This is of special importance in connection with saturation (see section 5). Weiss [49] has pointed out that partons with moderate momentum fraction in the proton have a rather narrow impact parameter profile and presented ideas how this might be used in studies of pp collisions at the LHC [50].

The exclusive production of vector mesons can also be studied in ultra-peripheral heavy ion collisions at RHIC. STAR presented [51] results on diffractive ρ^0 production in Au+Au and d+Au collisions, where a quasi-real photon emitted by one nucleus scatters quasielastically off the other nucleus and becomes a vector meson. STAR has studied samples where the interacting nuclei either stay intact or dissociate because of nuclear excitation, which leads to decay neutrons that are used to tag interactions at smaller impact parameter. The ρ^0 mass peak (Figure 14) observed by STAR is similar in shape to ρ^0 photoproduction at HERA, and the rapidity distribution matches a soft Pomeron model calculation. The t dependence in Au+Au collisions is found consistent with an interference effect due to the two indistinguishable production diagrams. The exponential t slope parameter $b \approx 11.5$ GeV^{-2} obtained in d+Au collisions where the deuteron dissociates is similar to values measured in scattering off the proton at HERA.

A theoretical study of the role of multiphoton exchange in lepton pair production in heavy-ion collisions has been presented by Kuraev [52].

5 Saturation

A significant fraction of theoretical contributions in the working group was devoted to saturation. They were presented in a common session with the working group on structure functions and low x, which was complemented by a discussion session. Studies oriented towards phenomenology are reviewed in this section, whereas more theoretical work is summarized in [53].

A point of view expressed by several participants in the discussion session is that the phenomenological success of colour dipole models in describing HERA data does *not* imply that the relevance of saturation dynamics in HERA kinematics has been firmly established. In this context it is important to distinguish between the breakdown of the leading-twist (or "DGLAP") description, the onset of BFKL dynamics, and the onset of saturation, by which we understand dynamics involving nonlinear effects, strong gluon fields, and unitarisation of the scattering amplitude. In the colour dipole formulation, saturation becomes relevant for dipoles of size $r \gtrsim 1/Q_s$, where Q_s is the saturation scale. Typical dipole sizes $r \sim 1/Q$ are selected by the momentum scale Q of the process in question. It was felt by several participants that to establish saturation convincingly, one needs processes where Q is below Q_s but at the same time large enough to justify the use of perturbation theory in the calculation. Unfortunately, the strongest effects of saturation are often found for Q^2 so small that the internal consistency of perturbative arguments is not evident. An example of such a situation is the study of high-mass diffractive photon dissociation presented by Munier [54]. As an indicator of how sensitive a calculation is to nonperturbative effects (and hence of the extent to which one goes from theory to modelling) one may for instance take the sensitivity of observables on the light quark mass which is often included in the $q\bar{q}$ wave function of the photon. This was done in a study presented by Rogers [55], which in the framework of a dipole model estimated that saturation effects are only of little importance in the inclusive structure function F_2 at $x_B = 10^{-4}$ and $Q^2 = 2$ GeV^2, to give a concrete kinematical point [56].

An important point is that the saturation scale Q_s depends not only on the energy variable $1/x$ but also on the impact parameter b of the scattering process. Whereas inclusive observables such as the structure functions F_2 and F_L average over all impact parameters, processes where the proton remains intact, like open diffraction, vector meson production, or DVCS offer the possibility to select the region of small impact parameters (corresponding to large t). In this region the gluon density in a proton is highest so that saturation will set in earlier at a given x. It is a renewed task for theory to indicate which processes and kinematics are most favorable in terms of sensitivity to saturation, of theoretical control, and of experimental feasibility.

To include impact parameter dependence in the theoretical description of saturation is challenging. Investigations of this dependence are at a rather early stage, and often it is still neglected altogether (see [53]). This also holds for the work reported by Utermann [57], where the large gluon fields involved in saturation are described by QCD instantons [58], thus providing a new implementation of the idea that high-energy scattering can be linked with fundamental properties of the QCD

vacuum.

6 Future Opportunities

Studies of diffractive phenomena represent an active field in experimental particle physics at present as well as future hadronic colliders. Both HERA and the TEVATRON are currently in their "Run 2" phases with upgraded detectors, for example the new H1 Very Forward Proton Spectrometer VFPS [59], which provides full acceptance for elastic protons in the diffractive regime around $x_{I\!P} \sim 0.01$, or the new D0 Roman Pot system [28]. A wealth of precise data is still expected from these experiments.

In 2007, the Large Hadron Collider LHC is scheduled to start operation at CERN, providing pp collisions at 14 TeV centre-of-mass energy. There are plans for diffractive studies using both omni-purpose LHC experiments, ATLAS and CMS. The TOTEM collaboration [60] will install additional detectors around the CMS interaction point, providing acceptance up to very large rapidities: two tracking telescopes T1 and T2 for measurements of forward particle production, which will cover $3.1 < \eta < 4.7$ and $5.3 < \eta < 6.5$, and a set of Roman Pot spectrometers between $z = 147$ m and $z = 220$ m on either side of the interaction point. The physics objectives [61] of TOTEM in standalone mode (without the CMS central detector) are a measurement of the pp elastic scattering cross section $d\sigma/dt$ in the range $10^{-3} < |t| < 10$ GeV^2 and the extraction of the total cross section at 14 TeV with an uncertainty of 1% using the optical theorem. These measurements require only a few days of LHC running (not taking into account commissioning) with a special high $\beta^* = 1540$ m optics at low luminosity $\mathcal{L} = 10^{28}$ cm^{-2}s^{-1}. In this configuration, about 90% of all diffractive protons are seen in the Roman Pots, their momentum being measurable with a resolution around 10^{-3}.

For the nominal LHC optics ($\beta^* = 0.5$ m) and design luminosity $\mathcal{L} > 10^{33}$ cm^{-2}s^{-1}, there is a full diffractive physics programme of TOTEM together with CMS [62], with TOTEM being fully integrated into the CMS trigger and data acquisition system as a CMS subdetector, in particular providing an L1 trigger signal from the Roman Pots. The programme includes single and double diffraction, hard diffraction with jets, Ws, or heavy quarks, search for diffractive SM or SUSY Higgs production and other new physics, as well as studies of low-x dynamics in the forward region [63]. The acceptance region in $x_{I\!P}$ for the Roman Pots at 220 m is $0.02 < x_{I\!P} < 0.2$. The large centre-of-mass energy of the LHC provides an extension of the accessible kinematic range to probe the structure of the diffractive exchange to very low β as well as to high Q^2.

In recent years, the possibility of discovering the Higgs boson in double diffractive events at the LHC has gained significant interest, because it provides in principle a clean process with a good signal over background ratio, with the potential of a precise mass reconstruction using the Roman Pots. However, to discover a light SM or MSSM Higgs, additional Roman Pot detectors need to be installed at $z = 320$ and/or $z = 420$ m to provide the necessary acceptance at low $x_{I\!P}$. Unfortunately, this would require installation in the cold section of the LHC machine as well as more sophisticated trigger scenarios since the Pots would be too far away

from the interaction region in order to provide an L1 trigger in time. The possible installation of these additional Pots as well as other scenarios are still under investigation.

A detailed analysis of diffractive Higgs production has been presented by Royon [64], where model predictions for signal and background reactions were at the basis of simulations for the CMS+TOTEM detector setup. Critical issues for finding a standard model Higgs identified in this study are triggering, cuts to enhance the signal to background ratio, and the resolution in the missing mass of the central system measured by the Roman pots.

The signal cross section used in the study of the Saclay group [64] are in overall agreement with those presented by Martin [65], who gave an overview of the theory developed by the Durham group to describe diffractive Higgs production and similar processes in hadron-hadron collisions. The generalized gluon distribution (see section 4) is an essential ingredient in this approach. As the Higgs would be detected in its $b\bar{b}$ decay mode, a major background to its observation is the diffractive production of $b\bar{b}$ pairs via two-gluon fusion, which can be described in the same theoretical framework. The study of exclusive dijet events, $p\bar{p} \to p + \mathrm{dijet} + \bar{p}$ at the TEVATRON can provide valuable checks of theory approaches. This is especially important since the description of rapidity gap survival has to rely on phenomenological models.

The ATLAS collaboration [66] has very recently submitted a Letter of Intent [67] for the installation of additional forward detectors, aimed at a precise luminosity determination. Since the ATLAS detector does not have sufficient forward coverage to measure the total inelastic rate precisely enough, the collaboration follows a different approach than TOTEM, namely using the very challenging method of Coulomb scattering. It is planned to install Roman Pot detectors at $z = 240$ m on either side of the ATLAS main detector in order to measure elastic protons in the Coulomb region at very small $|t| < 5 \cdot 10^{-4}$ GeV^2 during a special high β^* optics LHC run at low luminosity. This determination of the absolute luminosity, which is planned to be precise within less than 2%, would then be used to calibrate a luminosity monitor ("Lucid") based on Cerenkov counters placed around the beam pipe close to the interaction point, which would provide luminosity measurements for the standard LHC running. In the future, this programme will be extended to also cover diffractive and low-x physics, similarly to the CMS+TOTEM plans.

7 Conclusions

Diffraction has proven to be a healthy field at this workshop, with theoretical activity on a wide range of issues, and data that brought significant improvement over previous results or represented altogether new measurements. Preparation of studying diffractive physics at the LHC is well under way.

Acknowledgements

We thank all participants in our session for the excellent presentations and the lively discussions. Special thanks are due to Anna Stasto for co-organizing the common

session on saturation and to Larry McLerran for animating the discussion session on that topic. The organisers of DIS 2004 deserve credit for an enjoyable and very well organised meeting in pleasant surroundings.

References

1. M. Kapishin, *these proceedings*.
2. M. Ruspa, *these proceedings*.
3. H1 Collab., papers 088, 089 and 090 subm. to EPS 2003, Aachen.
4. H1 Collab., paper 984 subm. to ICHEP 2002, Amsterdam.
5. ZEUS Collab., papers 538 and 540 subm. to EPS 2003, Aachen.
6. J. Collins, *Phys. Rev.* **D 57** (1998) 3051 [erratum-ibid. **D 61** (2000) 019902].
7. ZEUS Collab., *Nucl. Phys.* **B 672** (2003) 3.
8. K. Wichmann-Klimek, *these proceedings*.
9. R. Sacchi, *these proceedings*.
10. ZEUS Collab., subm. to *Phys. Lett.* **B**, hep-ex/0404002.
11. ZEUS Collab., paper 544 subm. to EPS 2003, Aachen.
12. CDF Collab., *Phys. Rev. Lett.* **84** (2000) 5043.
13. S. Schätzel, *these proceedings*.
14. H1 Collab., paper 113 subm. to EPS 2003, Aachen.
15. N. Vlasov, *these proceedings*.
16. ZEUS Collab., *Nucl. Phys.* **B 672** (2003) 3.
17. S. Kagawa, *these proceedings*.
18. H1 Collab., *Z. Phys.* **C 76** (1997) 613.
19. H1 Collab., paper 087 subm. to EPS 2003, Aachen.
20. G. Kramer, *these proceedings*.
21. A. Kaidalov, V. A. Khoze, A. D. Martin, M.G. Ryskin, *Phys. Lett.* **B 567** (2003) 61.
22. H1 Collab., paper 6-0177 subm. to ICHEP 2004, Beijing.
23. ZEUS Collab., paper 6-0249 subm. to ICHEP 2004, Beijing.
24. ZEUS Collab., paper 547 subm. to EPS 2003, Aachen.
25. J. Ukleja, *these proceedings*.
26. K. Terashi, *these proceedings*.
27. A. Bialas, *these proceedings*.
28. T. Edwards, *these proceedings*.
29. F. Ellinghaus, *these proceedings*.
30. A. Borissov, *these proceedings*.
31. E. Kabuss, Summary of Working Group F: Spin Physics, *these proceedings*.
32. M. Helbich, *these proceedings*.
33. A. Bruni, *these proceedings*.
34. ZEUS Collab, S. Chekanov *et al.*, subm. to *Nucl. Phys.* **B**, hep-ex/0404008.
35. L. Szymanowski, *these proceedings*.
36. D. Ivanov, A. Schäfer, L. Szymanowski, G. Krasnikov, *Eur. Phys. J.* **C 34** (2004) 297.
37. J. Olsson, *these proceedings*.
38. H1 Collab., *Phys. Lett.* **B 568** (2003) 205.

39. ZEUS Collab., *Eur. Phys. J.* **C 26** (2003) 389.
40. L. Motyka, *these proceedings*.
41. R. Enberg, J. R. Forshaw, L. Motyka, G. Poludniowski, JHEP **0309** (2003) 008 and JHEP **0312** (2003) 002.
42. H1 Collab., paper 110 subm. to EPS 2003, Aachen.
43. A. V. Belitsky, D. Müller, A. Kirchner, *Nucl. Phys.* **B 629** (2002) 323.
44. H1 Collab., *Phys. Lett.* **B 517** (2001) 47.
45. ZEUS Collab., *Phys. Lett.* **B 573** (2003) 46.
46. L. Favart, *these proceedings*.
47. H1 Collab., paper 110 subm. to EPS 2003, Aachen.
48. L. Favart, *these proceedings*.
49. C. Weiss, *these proceedings*.
50. L. Frankfurt, M. Strikman, C. Weiss, *Phys. Rev.* **D 69** (2004) 114010.
51. A. Ogawa, *these proceedings*.
52. E. Kuraev, *these proceedings*.
53. A. Stasto, Theory Summary of Working Group A: Structure Functions and Low x, *these proceedings*.
54. S. Munier, *these proceedings*.
55. T. Rogers, *these proceedings*.
56. T. Rogers, V. Guzey, M. Strikman, X. Zu, *Phys. Rev.* **D 69** (2004) 074011.
57. A. Utermann, *these proceedings*.
58. F. Schrempp and A. Utermann, *Phys. Lett.* **B 543** (2002) 197.
59. X. Janssen, *these proceedings*.
60. M. Deile, *these proceedings*.
61. TOTEM Collab.: "Technical Design Report", CERN-LHCC-2004-002.
62. M. Taševský, *these proceedings*.
63. CMS Collab.: "Expression of Interest" (on diffractive and forward physics with TOTEM), LHCC-2004-003/G-068.
64. C. Royon, *these proceedings*.
65. A. D. Martin, *these proceedings*.
66. M. Boonekamp, *these proceedings*.
67. ATLAS Collab.: "Forward detectors for luminosity measurement and monitoring", CERN-LHCC-2004-010.